

A Column Generation Approach to the Discrete Barycenter Problem

Steffen Borgwardt¹ and Stephan Patterson²

¹ steffen.borgwardt@ucdenver.edu; University of Colorado Denver

² stephan.patterson@ucdenver.edu; University of Colorado Denver

Abstract. The minimum-cost mass transport problem for a set of discrete probability measures, called the discrete barycenter problem, can be solved exactly using exponential-sized linear programs. In applications, the support sets of the probability measures have two common settings that exhibit the extremes of the problem's complexity: all support points lie on the same regular grid, or all support points are unique and dispersed without structure. In the first, best-case setting, the discrete barycenter problem is well understood and solvable through a polynomial-sized linear program. We are interested in the second, worst-case setting, in which the underlying linear program is exponential in the number of variables, but contains an extremely low number of constraints, making it a prime candidate for column generation.

In this paper, we devise a column generation strategy for this setting through a Dantzig-Wolfe decomposition of the underlying linear program. We produce an efficiently solvable pricing problem – a classical transportation problem – by assigning all constraints associated with exactly two measures to the pricing problem. We give a vertex formulation for the master problem, and describe two efficient methods for constructing an initial feasible restricted master problem. Further, we use the structure of the constraints for a memory-efficient implementation of both the pricing and the master problem. We conclude with some computational experiments, demonstrating significant improvement in the memory requirements and running times compared to a computation using the full linear program.

Keywords: discrete barycenter, optimal transport, linear programming, column generation
MSC 2010: 49M27, 90B80, 90C05, 90C08, 90C46

1 Introduction

The discrete barycenter problem is: Given a set of probability measures P_1, \dots, P_n , each with a finite set $\text{supp}(P_i)$ of support points in \mathbb{R}^d , and a set of n non-negative weights $\lambda_i \in \mathbb{R}$ with $\sum_{i=1}^n \lambda_i = 1$, find a probability measure \bar{P} which minimizes the total squared Wasserstein distance to all given measures. Since P_1, \dots, P_n have finite sets of support points, the measures are called *discrete*. Because P_1, \dots, P_n are discrete, the solution measure \bar{P} , i.e., the *barycenter*, also has a finite set of support points, the Wasserstein distance is the squared Euclidean distance, and the problem can be solved exactly by linear programming [1, 2, 6, 16]. The computational complexity of the problem is open; all known LP formulations may require an exponential number of variables, scaling by the product of the sizes of the support sets of the input measures [5]. Some formulations also have an exponential number of constraints.

In this paper, we explore a column generation strategy for computing an exact solution to the discrete barycenter problem. In addition to the inherent benefit of an exact solution and its necessity for evaluation of the quality of heuristic approaches, exact barycenters also have favorable properties, namely, provable sparsity of the support set, and the *non-mass-splitting* property [1,2]: the mass of each barycenter support point is transported fully to a single support point in each measure. This non-mass-splitting property is fundamental to the modeling of many physical applications where such a split would be infeasible.

As applications for the barycenter problem appear in a variety of fields, including economics, physics, statistics, and game theory, significant effort continues on exact, approximate, and heuristic strategies to address the computational difficulties [17,18,19]. For a recent, thorough review of the Wasserstein distance and optimal transport from a statistical point of view, see [14]. State of the art approximation methods solve the entropy regularized optimal mass transport problem [8]. Entropic regularization leads to a strongly convex program, and its smoothing effects give qualitatively different solutions, notably, with dense support [3]. Entropy regularized transport problems can be solved efficiently, with a linear-in- n complexity bound, using iterative Bregman projection algorithms [3,9,15] or accelerated-gradient-descent-based algorithms [12]. The entropy regularization factor needs to be chosen proportional to the desired accuracy of the approximation’s transport value. Since the complexity of these approximation algorithms is inversely proportional to both the regularization factor and the desired accuracy, this is a source of numerical instability [12].

Model for the Discrete Barycenter Problem. Since the non-mass-splitting property holds for all (exact) barycenters, each support point in a barycenter is associated with a single combination of input support points, consisting of the points to which its mass is transported. The set of combinations of input support points is denoted $S^* = \{(\mathbf{x}_1, \dots, \mathbf{x}_n) : \mathbf{x}_i \in \text{supp}(P_i) \text{ for } i = 1, \dots, n\}$, with elements $s_h = (\mathbf{x}_1^h, \mathbf{x}_2^h, \dots, \mathbf{x}_n^h)$, $h = 1, \dots, |S^*|$. Each combination s_h has an associated *weighted mean* $\mathbf{x}^h = \sum_{i=1}^n \lambda_i \mathbf{x}_i^h$. The weighted mean \mathbf{x}^h is the optimal location for joint mass transport to the points in the combination s_h . Therefore the set S of distinct weighted means contains *all possible support points* for the barycenter.

Structure of Measures. When each combination s_h produces a different weighted mean \mathbf{x}^h , we say the measures P_1, \dots, P_n are in *general position*. When the measures P_1, \dots, P_n are instead *structured*, (significant) repetition in weighted means occurs. This beneficial repetition gives a smaller set of distinct weighted means S ; for grid-structured data, S contains orders of magnitude fewer elements than S^* .

Using $|P_i|$ to denote the size of the support set of P_i , the number of distinct \mathbf{x}^h for general position measures is $|S^*| = \prod_{i=1}^n |P_i|$; thus the number of weighted means is exponential in the number of input measures n . This is the worst-case scenario for the number of possible support points for \bar{P} . We provide an example of a discrete measure in \mathbb{R}^2 in Figure 1 (left), and three measures in general position in Figure 1 (right). Verifying the three measures are in general position is elementary but somewhat tedious, as the weighted means of all 27 combinations of support points must be computed and verified as unique. A barycenter for these measures is displayed in Figure 2 (left), shown with associated transport in Figure 2 (right).

Linear Programs for the Discrete Barycenter Problem. In this paper, we use an LP formulation from [5] based on S^* and chosen because, among known LP formulations, it requires the fewest variables and constraints for general position measures. For structured measures, duplication of \mathbf{x}^h creates a smaller set S , which can be used in a different type

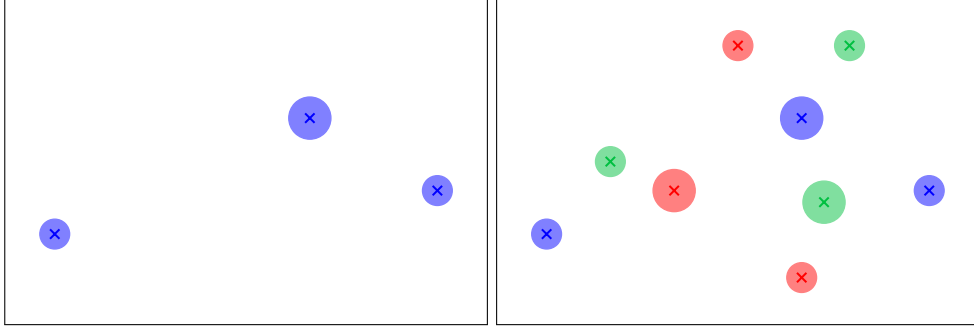


Fig. 1. (left) A discrete probability measure in \mathbb{R}^2 with three support points. The size of the points indicates their associated mass. (right) Three measures in \mathbb{R}^2 each with three support points. All combinations $(\mathbf{x}_1, \mathbf{x}_2, \mathbf{x}_3)$ produce a different weighted mean; therefore these measures are in general position.

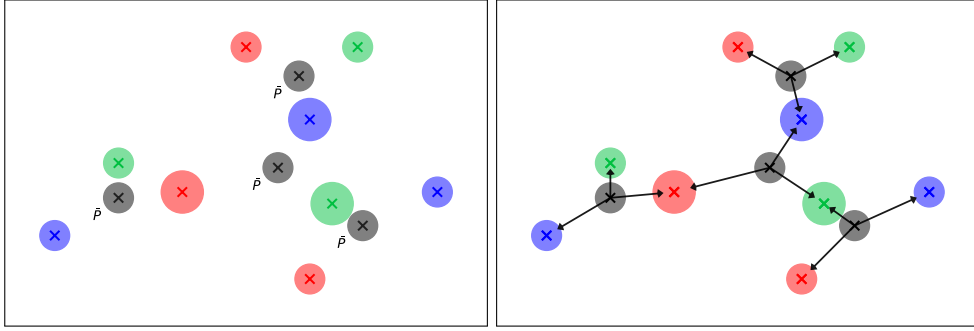


Fig. 2. (left) Assuming $\lambda_i = \frac{1}{3}$ for $i = 1, 2, 3$, a barycenter \bar{P} for the three measures from Figure 1. Each support point has mass $\frac{1}{4}$. (right) The mass transport from each barycenter support point to the original measures. Each barycenter support point is the weighted mean of the points to which it transports.

of LP formulation that performs better in this simpler setting. Details of both types of LP formulations are presented in [5].

We briefly describe the LP formulation based on S^* . A variable is introduced for each combination of support points; that is, each s_h has a corresponding variable w_h representing the mass assigned to \mathbf{x}^h and transported fully to each \mathbf{x}_i^h , $i = 1, \dots, n$. The total transport cost of a unit of mass from \mathbf{x}^h is given by $c_h = \sum_{i=1}^n \|\mathbf{x}^h - \mathbf{x}_i^h\|^2$. The objective of the LP formulation is a minimization of the total mass transport cost.

Constraints arise from the requirement that the total transport to each support point in each measure is exactly equal to its mass d_i . This produces one equality constraint for each \mathbf{x}_i ; that is,

$$\sum_{h: \mathbf{x}_i^h = \mathbf{x}_i} w_h = d_i, \quad \forall i = 1, \dots, n, \quad \forall \mathbf{x}_i \in \text{supp}(P_i).$$

The constraints can be represented as a real $\sum_{i=1}^n |P_i| \times \prod_{i=1}^n |P_i|$ matrix A times the vector w . In A , column h contains ones in the n rows where $\mathbf{x}_i^h = \mathbf{x}_i$, and zeroes otherwise. The matrix A is highly structured, a crucial property for an efficient column generation implementation. We postpone the analysis of A to Section 2. With c as the vector of costs c_h and w as the vector of variable masses w_h , a linear program for the discrete barycenter problem is:

$$\begin{aligned} \min \quad & c^T \mathbf{w} \\ \text{s.t.} \quad & A\mathbf{w} = d \\ & \mathbf{w} \geq 0. \end{aligned} \tag{general}$$

We choose to explore a column generation strategy due to the dimensions of A : the number of rows is $\sum_{i=1}^n |P_i|$, while the number of columns of A , and the number of variables in LP (general), is $\prod_{i=1}^n |P_i|$. Thus, the number of constraints scales linearly, equal to the total number of support points in the input measures. Meanwhile, the number of variables scales exponentially in the number of input measures.

Column Generation. As a service to the reader, we briefly recall the basics of a column generation strategy for solving a linear program. The process begins with partitioning the constraint matrix as $A = \begin{bmatrix} A_p \\ A_m \end{bmatrix}$. A preselected number of rows are assigned to the matrix A_p for use in a separate *pricing problem*. The pricing problem must contain enough information for its solution to be meaningful, but also remain sufficiently simple to be efficiently solvable. In Section 2, we discuss how we achieve this balance for the barycenter problem.

The remaining rows of A are assigned to the matrix A_m for use in a version of LP (general) called the *master problem*. The master problem already has fewer constraints than LP (general) due to the relocation of A_p to the pricing problem, but the primary reduction in size is achieved by restricting the number of columns in the linear program. The resulting linear program is called the *restricted master problem*.

We implement the restricted master problem using a Dantzig-Wolfe formulation [7] for LP (general); for background on this classic linear programming formulation see, for example, [10]. In LP (general), the bound on the elements of d guarantee the values of \mathbf{w} are in $[0, 1]$, so that the feasible region is a bounded polytope and can be expressed in terms of its vertices. Let V represent the set of vertices \mathbf{p} of the polytope $\{\mathbf{w} \in \mathbb{R}^d : A\mathbf{w} = d, \mathbf{w} \geq 0\}$. Using a subset of V of size J , that is, $\{\mathbf{p}_1, \dots, \mathbf{p}_J\}$ with $1 \leq J \leq |V|$, and variables μ , a restricted master problem LP (RM) is as follows.

$$\begin{aligned} \min \quad & \sum_{j=1}^J (c^T \mathbf{p}_j) \mu_j \\ \text{s.t.} \quad & \sum_{j=1}^J (A_m \mathbf{p}_j) \mu_j = d_m \\ & \sum_{j=1}^J \mu_j = 1 \\ & \mu_j \geq 0, \forall j = 1, \dots, J \end{aligned} \tag{RM}$$

The structure that makes LP (general) a prime candidate for column generation is preserved in LP (RM): the number of constraints remains low, $\sum_{i=1}^n |P_i| + 1$, as LP (RM) has just one additional constraint for convexity. Ideally, only a fraction of the total number of vertices are used in LP (RM), so that the number of columns and variables remains low.

This is the purpose of the pricing problem: to generate meaningful columns for introduction to LP (RM). The current optimum of LP (RM) – specifically, the dual solution – is used in the objective of the pricing problem to find new columns that may lead to a better optimum when included in LP (RM). Column generation terminates when the optimal value of the pricing problem is no longer negative.

Starting a column generation process requires an initial feasible LP (RM). To satisfy this requirement, two algorithms which produce a vertex of $\{\mathbf{w} \in \mathbb{R}^d : A\mathbf{w} = d, \mathbf{w} \geq 0\}$ are presented in Section 3. Section 4 contains computational experiments demonstrating the practical advantages of our column generation algorithm over direct computations using LP (general). We finish with some concluding remarks in Section 5.

2 Pricing Problem

An efficiently solvable pricing problem is key to successful column generation. In this section, we exploit two beneficial aspects of the discrete barycenter problem which lead to an efficient implementation: the structure of the coefficient matrix A , and the structure of the pricing problem that results from the choice of exactly two measures for A_p .

Recall that the pricing problem uses the current optimum of the restricted master problem to produce a new column to introduce to LP (RM). Specifically, the objective function of the pricing problem requires the dual solution to LP (RM), so let the dual solution be given by (\mathbf{y}, σ) , where \mathbf{y} is the real vector of size $\sum_{i=1}^n |P_i|$ containing the shadow prices associated with the mass transport constraints, and $\sigma \in \mathbb{R}$ is the shadow price associated with the convexity constraint, in LP (RM). Then the base form of the pricing problem is:

$$\begin{aligned} \min \quad & (c - \mathbf{y}^T A_m)^T \mathbf{p} + \sigma \\ \text{s.t.} \quad & A_p \mathbf{p} = d_p \\ & \mathbf{p} \geq 0. \end{aligned} \tag{price}$$

LP (price) is still an exponential-sized linear program: The constraint matrix A_p has an exponential number of columns, as does the matrix A_m , and the cost vector c has an exponential number of elements. In fact, LP (price) contains the same number of variables as LP (general). We now develop an improved pricing problem using information specific to the barycenter problem.

The Structure of the Coefficient Matrix A . Recall that A contains only elements 1 and 0: in column h , there is a 1 when \mathbf{x}_i is in the tuple s_h , that is, $\mathbf{x}_i^h = \mathbf{x}_i$, and 0 otherwise. In fact, each column contains exactly n nonzero coefficients. The pattern created within the matrix A is displayed in Example 1: each row has consecutive ones alternating with consecutive zeros. For each measure, the consecutive ones start in the first column for the first constraint in each measure, then start in the second row immediately after the end of the previous consecutive ones, continuing to the last constraint of the measure, forming a block. The width of the block depends on the measure P_i with which the constraints are associated. The number of consecutive ones equals the product of the sizes of the measures with a higher index: the rows of A associated with P_i , $1 \leq i < n$, contain $\prod_{l=i+1}^n |P_l|$ consecutive ones. The block for the final measure is the identity matrix.

Example 1. The matrix A for four measures with sizes $|P_1| = |P_3| = 2$ and $|P_2| = |P_4| = 3$ contains blocks of ones and zeros. The width of block structure for particular constraints depends on the index i of the corresponding measure P_i . Here there are 36 total columns, and the number of consecutive ones for each measure is 16, 6, 3, and 1, respectively.

Because A is easily generated, the matrix A_m is *not required in memory*. Instead, in the objective function, $\mathbf{y}^T A_m$ is calculated using the $|P_i|$ to determine which dual values should be added. For further computational efficiency, updates to elements of $(c - \mathbf{y}^T A_m)$ are only required for those values of \mathbf{y} which have changed from the previous iteration; due to the sparse nature of A_m , many elements may remain unchanged.

Input:

- Output: Column h of matrix A , denoted A_h

$$2: j = \lfloor \frac{h}{\prod_{l=2}^n |P_l|} \rfloor$$
3: $A_h(j) = 1$ 4: **for** $i = 2, \dots, n - 1$ **do**
$$5: \quad j = \sum_{l=1}^{i-1} |P_l| + \lfloor \frac{h \pmod{\prod_{l=i}^n |P_l|}}{\prod_{l=i+1}^n |P_l|} \rfloor$$

6: $A_h(j) = 1$

$$7: j = \sum_{l=1}^{n-1} |P_l| + h \pmod{|P_n|}$$
8: $A_h(j) = 1$

Example 2. Using the matrix A from Example 1, a decomposition of all constraints associated with the first two measures into the pricing problem gives this matrix A_p .

$$A_p = \begin{bmatrix} 1 & 1 & 1 & 1 & 1 & 1 & 1 & 1 & 1 & 1 & 1 & 1 & 1 & 1 & 1 & 1 & 0 & 0 & 0 & 0 & 0 & 0 & 0 & 0 & 0 & 0 & 0 & 0 & 0 & 0 \\ 0 & 0 & 0 & 0 & 0 & 0 & 0 & 0 & 0 & 0 & 0 & 0 & 0 & 0 & 0 & 0 & 1 & 1 & 1 & 1 & 1 & 1 & 1 & 1 & 1 & 1 & 1 & 1 & 1 & 1 \\ 1 & 1 & 1 & 1 & 1 & 1 & 0 & 0 & 0 & 0 & 0 & 0 & 0 & 0 & 0 & 0 & 1 & 1 & 1 & 1 & 1 & 0 & 0 & 0 & 0 & 0 & 0 & 0 & 0 & 0 \\ 0 & 0 & 0 & 0 & 0 & 0 & 1 & 1 & 1 & 1 & 1 & 0 & 0 & 0 & 0 & 0 & 0 & 0 & 0 & 0 & 0 & 1 & 1 & 1 & 1 & 1 & 0 & 0 & 0 & 0 & 0 \\ 0 & 0 & 0 & 0 & 0 & 0 & 0 & 0 & 0 & 0 & 0 & 1 & 1 & 1 & 1 & 1 & 0 & 0 & 0 & 0 & 0 & 0 & 0 & 0 & 0 & 1 & 1 & 1 & 1 & 1 & 1 \end{bmatrix}$$

Every column is repeated six times: $|P_3| \cdot |P_4|$. The matrix of unique columns is U_p .

$$U_p = \begin{bmatrix} 1 & 1 & 1 & 0 & 0 & 0 \\ 0 & 0 & 0 & 1 & 1 & 1 \\ 1 & 0 & 0 & 1 & 0 & 0 \\ 0 & 1 & 0 & 0 & 1 & 0 \\ 0 & 0 & 1 & 0 & 0 & 1 \end{bmatrix}$$

Replacing the constraint matrix A_p in LP (price) with the matrix of unique columns U_p requires a corresponding change to the objective function. Noting that LP (price) is the minimization of a linear objective, only the most negative coefficient for each unique column is required: in an optimal solution, all mass is assigned to such a column. Thus, it suffices to keep a best-cost vector b for the unique columns. These two substitutions produce LP (Uprice).

$$\begin{aligned} \min \quad & b^T \mathbf{q} + \sigma \\ \text{s.t.} \quad & U_p \mathbf{q} = d_p \\ & \mathbf{p} \geq 0. \end{aligned} \quad (\text{Uprice})$$

Using LP (Uprice) improves solvability and memory requirements in two major ways: when $k = 2$, LP (Uprice) requires just $|P_1| \cdot |P_2|$ variables, a tremendous reduction from $\prod_{i=1}^n |P_i|$. The number of variables *does not depend on n* . When the input measures have support sets of equal size $|P|$, this eliminates $|P|^{n-2}$ variables. Additionally, the constraint matrix is stored in memory, so the benefit of replacing A_p with U_p is significant.

Using LP (U**price**) instead of LP (**price**) requires additional preprocessing each iteration to construct the best-cost vector b , which does use the exponential-sized vector $(c - \mathbf{y}^T A_m)$. The preprocessing for LP (U**price**), repeated each iteration, is given in Algorithm 2. In particular, Algorithm 2 highlights the important selection of which indices h correspond to the unique columns used in LP (U**price**).

Algorithm 2 Setup of LP (Uprice)

Intialize the vector of indices I of length n_u

Update $a = c - y^T A_m$

for $j = 1, \dots, n_u$ **do****for** $h = 1 + n_d \cdot (j - 1), \dots, n_d \cdot j$ **do**

if $h = 1 + n_d \cdot (j - 1)$ **then**

$$b_j = a_h$$
$$I(j) = h$$

else

$$b_j = \min\{b_j, a_h\}$$
$$I(j) = h$$

Update objective of LP (Uprice)

Decomposition of Constraints for Exactly Two Measures. As in Example 2, we partition A with $k = 2$; that is, we always partition A where A_p , and subsequently the matrix of unique columns U_p , contains all rows of constraints associated with exactly two measures. LP (Uprice) has a linear objective function $b^T \mathbf{q} + \sigma$; because of the linear objective and the structure of the constraints for two measures, LP (Uprice) is a classical transportation problem [11,13], a special case of a minimum-cost flow problem. Therefore, LP (Uprice) can be solved in strongly polynomial time [2,5].

Theorem 1. *Let $U_p \mathbf{q} = d_p$ be the constraints associated with exactly two measures. Then LP (Uprice) is a classical transportation problem and can be solved in strongly polynomial time.*

Next, we turn to the restricted master problem, and describe two strategies for a feasible start.

3 Master Problem: Constructing a Vertex

The process of column generation begins with a restricted master problem, restated here for reference.

$$\begin{aligned}
\min \quad & \sum_{j=1}^J (c^T \mathbf{p}_j) \mu_j \\
\text{s.t.} \quad & \sum_{j=1}^J (A_m \mathbf{p}_j) \mu_j = d_m \\
& \sum_{j=1}^J \mu_j = 1 \\
& \mu_j \geq 0, \forall j = 1, \dots, J
\end{aligned} \tag{RM}$$

By design, column generation starts with a low number of variables, then introduces additional columns iteratively. Therefore, the size of the initial LP (RM) is small, and increases linearly with the number of columns generated.

Memory Usage and Setup of LP (RM). Once the column generation process has begun, the previous pricing problem produces a solution \mathbf{q} containing the nonzero elements of a new \mathbf{p}_J to be introduced to LP (RM). This \mathbf{q} has at most $|P_1| \cdot |P_2|$ nonzero elements. Recall from Section 2 that A_m is easily generated, so the pricing problem does not require A_m to be stored in memory. The restricted master problem also does not require A_m to be stored; instead, the $|P_i|$ are used to calculate the new column $A_m \mathbf{p}_J$. Combined with the small number of nonzero elements of \mathbf{p}_J , a computation of $A_m \mathbf{p}_J$, as well as of $c^T \mathbf{p}_J$, can be done efficiently.

For additional efficiency, the solver for LP (RM) uses the previous solution as a warm start. Using the primal simplex method then typically finds a new optimal solution in just a few simplex steps for each update of LP (RM).

We begin with a single column in LP (RM) by generating an initial \mathbf{p}_1 so that the first LP (RM) has feasible solution $v_1 = 1$, as required by the convexity constraint. Substituting into the other constraints, \mathbf{p}_1 must be a solution to $A_m \mathbf{p} = d_m$. Any feasible solution to the full system $A \mathbf{w} = d$ also contains a solution to the equalities $A_m \mathbf{p} = d_m$, so we can generate a vertex of either $A_m \mathbf{p} = d_m$ or the full system $A \mathbf{w} = d$. Generating a vertex of the full system has the benefit of starting with a potential optimum, and requires

little additional computational effort. We consider two methods for constructing a vertex of the polytope generated by the constraints $A\mathbf{w} = d$: a greedy construction and the 2-approximation algorithm from [4]. The following methods also work for $A_m p = d_m$ by simply limiting the input to the relevant constraints.

3.1 Feasibility through Greedy Construction

We first present an algorithm which greedily constructs a solution to $A\mathbf{w} = d$. The process begins by generating a combination $s_h = (\mathbf{x}_1^h, \mathbf{x}_2^h, \dots, \mathbf{x}_n^h) \in S^*$, then assigning to \mathbf{x}^h the maximum mass w_h that does not violate the non-mass-splitting property: the minimum mass not yet supplied to the support points \mathbf{x}_i^h . After marking the mass w_h as supplied, the process is repeated, generating the next combination. This process is given in Algorithm 3.

Algorithm 3 Greedy Construction of \mathbf{w} : $A\mathbf{w} = d$

Input: vector n_o containing number of consecutive ones for each i
Output: vector \mathbf{w}
Let $L = 1$, $m_1 = 0$, and $j_i = 1 \ \forall i = 1, \dots, n$
For each P_i , and for $j_i = 1, \dots, |P_i|$, let b_{ij_i} be the mass associated with support point \mathbf{x}_{ij_i}
1: **while** $\sum_{l=1}^L m_l < 1$ **do**
2: $m_L = \min\{b_{ij_i}\}$
3: $h = \sum_{i=1}^n ((j_i - 1)n_o(i))$
4: $w_h = m_L$
5: **for** $i = 1, \dots, n$ **do**
6: $b_{ij_i} = b_{ij_i} - m_L$
7: **if** $b_{ij_i} = 0$ **then**
8: $j_i = j_i + 1$
9: $L = L + 1$

Theorem 2. For n probability measures with fixed sizes $|P_1|, \dots, |P_n|$, Algorithm 3 runs in $\mathcal{O}(n^2)$ in the arithmetic model of computation.

Proof. Assume probability measures P_1, \dots, P_n have support sets of fixed size.

First, we show that the number of nonzero elements produced by Algorithm 3, which is also the number of repetitions of the loop of Algorithm 3, is between $\max_{1 \leq i \leq n} \{|P_i|\}$ and $\sum_{i=1}^n |P_i| - n + 1$. The lower bound, $\max_{1 \leq i \leq n} \{|P_i|\}$, is an immediate consequence of the non-mass-splitting property maintained by Algorithm 3. For the upper bound, $\sum_{i=1}^n |P_i| - n + 1$, note that the last iteration must fully supply the mass to n points, one \mathbf{x}_i from all P_i , because the total mass for each P_i is the same (one). In each previous iteration, the minimum number of support points whose index j_i changes is one, for a total of $\sum_{i=1}^n (|P_i| - 1) + 1 = \sum_{i=1}^n |P_i| - n + 1$ iterations.

By assumption, the sizes of the support sets $|P_i|$ do not depend on n , so the number of iterations of Algorithm 3 is linear in n . Since each step inside this loop of Algorithm 3 requires at most linear-in- n elementary operations, we obtain Theorem 2. \square

As an additional consequence of the iteration bound $\sum_{i=1}^n |P_i| - n + 1$, the number of nonzero mass elements of \mathbf{w} , and subsequently the relevant elements of \mathbf{w} that solve $A_m \mathbf{p} = d_m$, are also bounded. Therefore the setup of the first LP (RM) is efficient.

We now show that Algorithm 3 produces a vertex of the polytope generated by the constraints $A\mathbf{w} = d$.

Theorem 3. *Algorithm 3 generates a vertex of the polytope $\{\mathbf{w} \in \mathbb{R}^d : A\mathbf{w} = d, \mathbf{w} \geq 0\}$.*

Proof. Let A, d be given and let \mathbf{w} be generated using Algorithm 3. We show there exists a c such that \mathbf{w} is the unique optimal solution to:

$$\begin{aligned} \min \quad & c^T \mathbf{w} \\ \text{s.t.} \quad & A\mathbf{w} = d \\ & \mathbf{w} \geq 0. \end{aligned}$$

Let M be the set of nonzero elements of \mathbf{w} , with size $|M| = L$. Order the elements of M in order of construction by Algorithm 3, m_1, \dots, m_L . Also order the associated indices h_1, \dots, h_L as calculated by Algorithm 3. Let $c_{h_1} = 1, c_{h_2} = 2, \dots$, and $c_{h_L} = L$. Let all other c_h , those whose h -index is not in h_1, \dots, h_L , be $\sum_{i=1}^n |P_i| - n + 2$ (Recall: $|M| \leq \sum_{i=1}^n |P_i| - n + 1$).

By construction, removing mass from a combination with a lower index and assigning it to a combination with higher index in M , that is, from m_j to m_k with $j \leq k$, will strictly increase the value of $c^T \mathbf{w}$. This includes moving mass to a combination with no mass in \mathbf{w} , that is, with an index not in M .

So it suffices to show that mass cannot be reassigned from m_k to m_j , $j \leq k$. The mass m_j is chosen such that for at least one x_{j_i} , the mass d_{j_i} has been fully supplied. Therefore m_j cannot be increased without violating the constraints $A\mathbf{w} = d$.

Therefore \mathbf{w} minimizes $c^T \mathbf{w}$ subject to $A\mathbf{w} = d$, since the maximum mass allowable is assigned to the cheapest costs. Furthermore, \mathbf{w} does so uniquely, since any change in its elements will strictly increase the value of $c^T \mathbf{w}$ due to the construction of c . Therefore \mathbf{w} is a vertex. \square

In Figure 3 (left), we display an example with three measures, two with 10 support points and one with 11 support points. Each measure has equally distributed mass. Applying Algorithm 3 results in a feasible solution supported on 20 weighted means of varying mass, displayed in Figure 3 (right), along with the transport for three sample points.

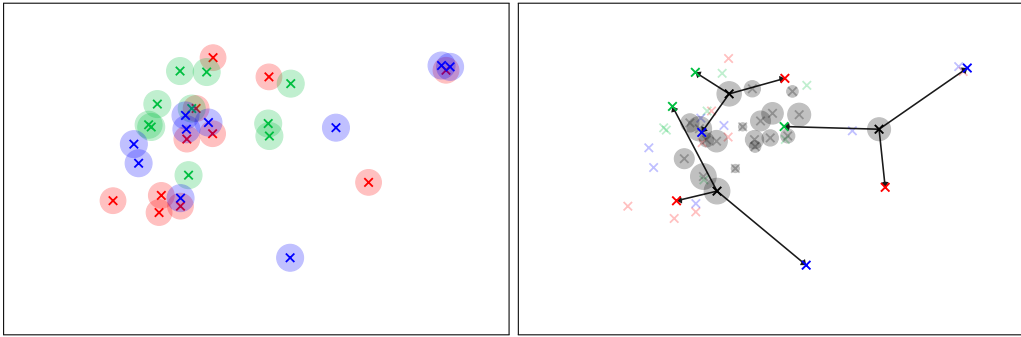


Fig. 3. (left) Three measures in general position with 10 or 11 support points and equally distributed mass. (right) A greedily constructed feasible solution. Transport from three sample points—those constructed first, fifth, and seventeenth—is shown (arrows). Each support point is the weighted mean of its three destination points.

3.2 Feasibility through a 2-Approximation

An alternative to the greedy-start algorithm, the provably efficient 2-approximation algorithm presented in [4], also generates a measure with feasible transport. The motivation for considering this algorithm is the guarantee that the generated transport cost is at most twice the optimal transport cost of a barycenter. This allows the examination of the effects of a feasible start of the column generation with a provably good initial objective value.

The non-optimal measure, called an *approximate barycenter*, is found by allowing mass to be placed only at the locations of the original support points, $\bigcup_{i=1}^n \text{supp}(P_i)$. The points in $\bigcup_{i=1}^n \text{supp}(P_i)$ are introduced to an alternative LP from [2,5]. This strategy avoids the possibly exponential number of weighted means by replacing them with the original support points. The approximate barycenter can be calculated in strongly polynomial time [4]. In Figure 4 (left), we show the result of this algorithm applied to the data set from Figure 3 (left). Mass is assigned to 15 of the 31 possible support points from the support sets of the original measures.

The approximate barycenter does not immediately translate to a solution to LP (general) for two reasons. One, this method of approximation does not maintain the non-mass-splitting property. Therefore a support point in the approximate barycenter may not correspond to a single combination $s_h \in S^*$. Two, even if a solution is non-mass-splitting, the points in $\bigcup_{i=1}^n \text{supp}(P_i)$ are typically not weighted means of any combination s_h .

Fortunately, the same process as in Algorithm 3 can address both of these issues. When applied to an approximate barycenter, Algorithm 3 corresponds to the iterative improvement process presented in [4]. Each support point in the approximate barycenter is processed as follows: first, a combination in S^* is created by collecting one point from each measure to which the support point transports mass. Then, the minimum of the mass available from the support point of the approximate barycenter and the smallest mass still required by the destination points is assigned to the combination. Applying Algorithm 3 to Figure 4 (left) results in a measure whose support set contains 24 weighted means, displayed in Figure 4 (right).

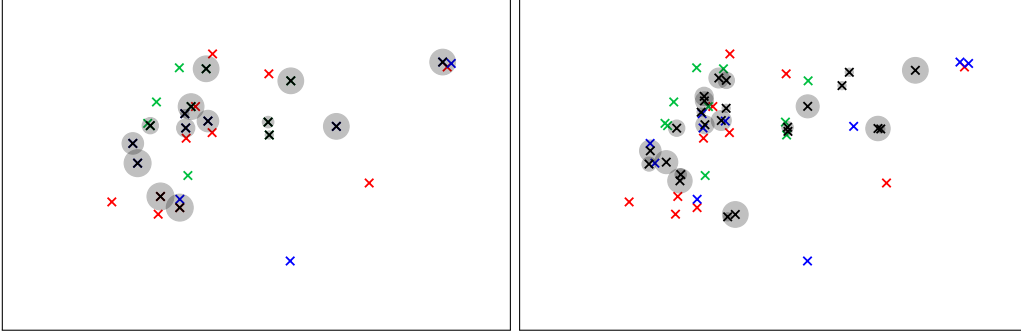


Fig. 4. (left) For the measures of Figure 3, the support of the measure produced by the two-approximation algorithm consists of 15 of the original support points. (right) Each support point in (left) is processed by Algorithm 3 to regain the mass-splitting property. The new support points are weighted means.

4 Computations

In our experiments, we use event locations from a real-world data set given in longitude and latitude coordinates. Because the event locations occur without known structure, probability measures with these support points are in general position. All computations have been run on a laptop (MacBook Pro, 2.9 GHz Intel Core i7, 16 GB of RAM, SSD). Data processing and the setup of the LPs were implemented in C++ and the LPs were solved using Gurobi 8.0. The source code is available at <https://github.com/StephanPatterson/Barycenter-Formulations>.

We implemented six variants of column generation for the barycenter problem, three using Algorithm 3, *greedy-start*, and three using the 2-approximation algorithm [4], *2-app-start*, to generate the initial vertex. All implementations that use the same initialization algorithm begin with the same vertex.

As described in Section 2, the constraints from two measures are assigned to the pricing problem. Our implementations differ in which two measures are chosen: we consider three options based on the size of the support sets. The variants labeled *large* choose the two measures with the largest support sets, resulting in a large pricing problem and small restricted master problem. The *small* variants choose the two measures with the smallest support sets, resulting in a small pricing problem and large restricted master problem. Finally, the *any* variants just use the first two input measures for the pricing problem, regardless of size; essentially, an arbitrary pair of measures. The choice of the pairs of measures is independent of the initialization strategy.

We begin with a comparison of our column generation implementations to a direct solution of LP (*general*). We consider measures with a small number of support points, because even with these small support sizes, using LP (*general*) already requires millions of variables (throughout this section, we will use this number to reference a particular instance). The

	LP (general)		Greedy-start					
			Any		Large		Small	
n	Variables	Time (sec)	Iter	Time (sec)	Iter	Time (sec)	Iter	Time (sec)
12	55,296	0.48	132	0.19	172	0.19	198	0.31
12	138,240	1.25	239	0.79	307	0.93	300	3.51
12	1,990,656	23.17	356	9.75	541	13.37	331	10.75
12	2,177,280	20.32	478	18.21	541	13.61	229	19.48
14	2,654,208	36.49	328	15.71	694	22.00	328	21.69
13	3,981,312	42.29	459	23.44	598	28.85	340	23.19
15	18,579,456	229.17	399	133.60	704	150.86	489	226.80
12	25,288,704	592.70	640	213.74	541	144.28	416	191.21
14	28,440,792	1029.42	545	252.37	854	276.13	425	312.28
14	32,514,048	1248.36	601	240.06	575	217.16	450	375.66
14	37,933,056	*	759	362.06	618	268.33	479	427.34
14	75,866,112	*	595	938.63	514	454.45	466	902.17
16	130,056,192	*	513	1265.87	872	1306.86	559	1950.79
14	151,732,224	*	823	1713.78	710	1307.42	559	1625.01

Table 1. Comparison of greedy-start algorithms for n measures per experiment, with fastest times in bold. Each measure has a small number (between 2 and 12) of points in general position. For larger instances, a direct solution was not possible due to memory constraints (*).

number of iterations for all variants also represents the number of variables introduced in the restricted master problem. We will conclude with some experiments using larger support sets, which cannot be solved using LP ([general](#)) due to memory constraints.

Small Measures: Running Times. We begin with n measures, most of which contain two to four support points, with the largest containing twelve support points. In Table 1, we see that all implementations of greedy-start column generation outperform LP ([general](#)). For most instances, the total running time is about half of a direct solution of LP ([general](#)). The large-choice variant is typically fastest, followed by the any-choice variant. When any-choice is fastest, the running times of large-choice are usually comparable, and both are always better than a direct computation.

In Table 2, we display the same instances, now solved using the 2-app-start strategy. Again, all variants significantly outperform the direct solution of LP ([general](#)), and using the large-choice pricing problem typically performs well. The pricing problem that works best for each experiment is the same as for greedy-start in Table 1. Comparing the running times to the greedy-start variants, 2-app-start appears to perform better for small instances, but greedy-start performs better for large instances.

Small Measures: Memory Usage. The instances in Tables 1 and 2 show that, as expected, significantly larger barycenter problems are solvable using column generation. For the four largest instances, a direct computation through LP ([general](#)) is not possible due to memory constraints, but column generation variants reach a solution in only a few additional iterations over the smaller problem instances.

In fact, our algorithm requires orders of magnitude less memory. The six variants of column generation do not vary significantly in memory usage; a comparison of memory requirements is available in Table 3.

	LP (general)		2-app-start					
	Variables	Time (sec)	Any		Large		Small	
n			Iter	Time (sec)	Iter	Time (sec)	Iter	Time (sec)
12	55,296	0.48	116	0.18	54	0.09	131	0.20
12	138,240	1.25	179	0.46	253	0.59	137	0.54
12	1,990,656	23.17	381	9.71	806	19.99	327	10.96
12	2,177,280	20.32	586	19.60	601	15.61	212	17.55
14	2,654,208	36.49	312	13.71	428	13.75	365	23.40
13	3,981,312	42.29	623	30.55	816	38.77	384	26.97
15	18,579,456	229.17	429	149.30	881	185.47	428	194.71
12	25,288,704	592.70	745	264.90	536	157.27	474	214.33
14	28,440,792	1029.42	636	280.12	814	258.00	406	312.40
14	32,514,048	1248.36	660	277.50	549	204.41	491	407.67
14	37,933,056	*	974	448.53	581	254.73	507	446.64
14	75,866,112	*	690	1113.12	687	595.37	487	1031.18
16	130,056,192	*	554	1382.33	1169	1722.82	545	1886.52
14	151,732,224	*	1020	2050.50	1016	1771.51	671	2084.94

Table 2. Comparison of 2-app-start algorithms for n measures per experiment, with fastest times in bold. Each measure has a small number (between 2 and 12) points in general position. For larger instances, a direct solution was not possible due to memory constraints (*).

LP (general)		Column Generation
1,990,656	3.70 GB	95 MB
2,177,280	4.00 GB	95 MB
2,654,208	4.97 GB	114 MB
3,981,312	7.14 GB	164 MB
18,579,456	45.2 GB	724 MB
25,288,704	49.6 GB	977 MB
28,440,792	54.8 GB	1.08 GB
32,514,048	62.7 GB	1.23 GB

Table 3. For the instances of Tables 1 and 2, the reduction in memory required is dramatic.

Step	Percentage of Computation Time
Setup LP (RM)	< 0.1%
Solve LP (RM)	1.1%
Update $(c - \mathbf{y}^T A_m)$	72.5%
Calculate b	26.2%
Solve LP (Uprice)	< 0.1%

Table 4. Percentage computation time per step of an average iteration of column generation. Most of the effort is spent on the setup of LP ([Uprice](#)); the computation times for solving LP ([Uprice](#)) and the setup of the next LP ([RM](#)) contribute negligibly to the total.

Small Measures: Running Time Breakdown. Table 4 displays the percentage of time per iteration spent on each step of the column generation process. The majority of computation time is in the update of $(c - \mathbf{y}^T A_m)$. This is as expected in light of the discussion in Section 2: it is the only part of the iteration that still requires exponential effort, due to the exponential size of $(c - \mathbf{y}^T A_m)$.

The computational effort required for solving LP ([RM](#)) and LP ([Uprice](#)) is very small, relative to the effort required for the coefficient calculation. Since LP ([Uprice](#)) can be solved in less total time than LP ([RM](#)), assigning more constraints to LP ([Uprice](#)) instead of LP ([RM](#)) is beneficial to running times; however, LP ([RM](#)) also solves relatively quickly, so overall, using the large-choice variant has a minor beneficial effect on running times. This explains why the large-choice variants perform well, but not tremendously better than the other variants in settings where the measures are fairly uniform in size; we will see more differentiation between the large-choice and any-choice variants in later experiments.

Small Measures: Convergence. Finally, we measure the absolute error associated with the objective value of LP ([RM](#)) for each iteration. We see similar behavior in each experiment; in Figure 5 we give a representative graph. The 2-app-start begins with a lower error, as expected. However, starting with less error does not appear to reduce the number of required iterations to the final solution as the value does not begin to improve until after the iteration where the greedy-start strategies have reached similar error. All strategies begin with a phase where the objective value is unchanged. To explain this, we note that the \mathbf{p} produced by the pricing problem do not satisfy $A_m \mathbf{p} = d_m$, by construction. Several iterations are required to build up enough columns (degrees of freedom) for the restricted master problem to reallocate mass and start improving the objective value.

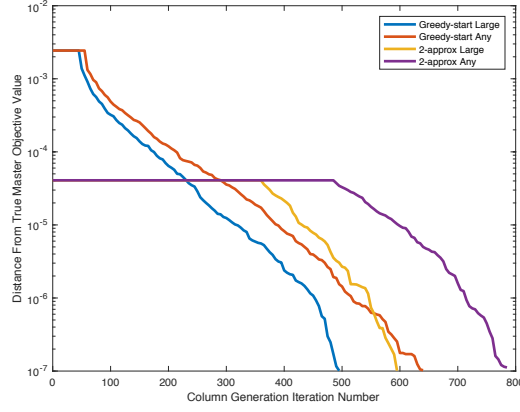


Fig. 5. A representative graph of the absolute error of the optimum of LP (RM), given by iteration. The 2-app-start begins with less error, but requires more iterations before improvement.

After this initial phase, the objective value does improve steadily, though there may still be consecutive iterations with the same value. For this reason, improvement in the objective value is not a feasible stopping criterion. This is similar to the behavior of the simplex method, where multiple iterations may be required to leave a degenerate vertex. In our experiments, we terminate when the pricing objective is above -10^{-6} . The corresponding true error is generally about 10^{-7} , as shown in Figure 5. Of course, higher tolerance levels for stopping the column generation algorithm could be used for earlier termination. For the experiment of Figure 5, each variant reaches an absolute error of 10^{-5} in approximately 150 fewer iterations than reaching an absolute error of 10^{-7} .

Two Measures of Larger Size. Next, we consider a few experiments for measures with larger support sets. In the previous experiments, Tables 1 and 2, all measures are roughly uniform in size, so the measures moved to the pricing problem in the large-choice variants are not significantly larger than the other measures. When there is a more dramatic difference in size, the benefit of using larger measures in the pricing problem is significant. Experiments

LP (general)		Greedy-start				2-app-start			
		Any		Large		Any		Large	
n	Variables	Iter	Time (sec)	Iter	Time (sec)	Iter	Time (sec)	Iter	Time (sec)
12	11,870,208	602	154.62	553	75.36	740	175.27	551	73.83
14	157,593,600	960	2268.26	745	1364.09	1456	3372.14	665	1223.45
14	163,897,344	883	3221.68	431	810.62	1191	4482.65	340	697.83
15	331,776,000	1081	5512.45	1024	3819.14	1683	8251.77	1017	3901.70

Table 5. When the two measures chosen for the pricing problem are significantly larger than the other input measures, the large-choice implementations are strongly advantageous. The largest two measures contain twenty to fifty support points, while all other measures still contain two to four support points. Fastest times are highlighted in bold.

Direct Solution		Greedy-start				2-app-start			
		Any		Large		Any		Large	
n	Variables	Iter	Time (sec)	Iter	Time (sec)	Iter	Time (sec)	Iter	Time (sec)
7	48,380,640	1475	796.60	1429	761.73	3406	1735.96	3501	1804.31
8	50,738,688	1287	724.94	1049	598.70	2406	1308.10	1893	1043.28
6	50,828,800	3004	1635.49	2553	1386.27	4050	2195.26	3808	2057.95
6	65,664,000	2845	2007.78	2883	2000.53	5142	3722.69	4848	3487.34
6	81,259,200	2627	2421.24	3993	3505.62	4388	3832.54	5906	5263.16
6	91,733,292	2360	2412.78	2694	2608.86	4436	4358.10	4716	4727.34

Table 6. These experiments use fewer measures (6-8), but each measure has larger support (10-30 points). The greedy-start strategy consistently outperforms the 2-app-start strategy, with fastest times highlighted in bold.

of this nature are shown in Table 5; here, the majority of the measures are the same size as in Tables 1 and 2, containing two to four support points. However, the largest two measures contain at least twenty support points, up to fifty points. In this setting, the 2-app-start slightly outperforms the greedy-start, and both benefit greatly from the large-choice partitioning.

Larger Measures of Uniform Size. We conclude our experiments by considering measures which all have larger support sets, 10-30 support points per measure. The resulting LP (general) is too large to solve on the laptop for all these instances. However, all implementations of column generation find a solution, with greedy-start outperforming 2-app-start column generation, shown in Table 6. This is not a result of generating the initial vertex; the 2-app-start and greedy-start initialization times remain small, at only a few seconds. Instead, we observe a significantly higher number of iterations in both 2-app-start variants. This may be due to the effect shown in Figure 5; 2-app-start implementations require many more iterations to begin improving on the initial objective value.

5 Concluding Remarks

Column generation performs well for the discrete barycenter problem with input data in general position, due to a structured constraint matrix and the ability to solve the pricing problem with a small linear program. Using this strategy, we have been able to significantly reduce the memory requirements for a linear programming approach to a barycenter problem, allowing for computations on much larger instances with significant improvements in total solution times. When an exact solution is desired, we recommend initializing column generation using Algorithm 3, and using the large-choice variant for the measures for the pricing problem. Further analysis would be required to better understand why starting column generation using the 2-approximation algorithm is outperformed by the simpler greedy algorithm. At this time, we believe it is more difficult for the approach to leave a “local optimum”, as generated by the 2-approximation algorithm.

Most algorithms for the discrete barycenter problem, LP-based or not, require an explicit specification of the whole set of support points that may be allocated mass in the computation of an approximate or exact barycenter. The size of this support set typically is a bottleneck for the practical performance. However, the existence of sparse solutions to the problem [2] indicates that strategies which dynamically introduce combinations s_h of

support points that may be assigned mass are promising. Essentially, the goal would be to generate columns of LP (general) directly; in this paper, we generated columns for a corresponding Dantzig-Wolfe formulation. An efficient generation of columns for LP (general) will require methods that are quite different from classical column generation strategies: While it is possible to find the shadow price for any given combination s_h , the challenge lies in finding a combination of best shadow price without an explicit evaluation of each combination in S^* .

Acknowledgments

We thank Ethan Anderes for the implementation of a visualization basis for barycenters used in [2], which we modified to produce the figures of Sections 1 and 3. We gratefully acknowledge support through the Collaboration Grant for Mathematicians *Polyhedral Theory in Data Analytics* of the Simons Foundation.

References

1. M. Agueh and G. Carlier. Barycenters in the Wasserstein space. *SIAM Journal on Mathematical Analysis*, 43(2):904–924, 2011.
2. E. Anderes, S. Borgwardt, and J. Miller. Discrete Wasserstein Barycenters: Optimal Transport for Discrete Data. *Mathematical Methods of Operations Research*, 84(2):389–409, 2016.
3. J.-D. Benamou, G. Carlier, M. Cuturi, L. Nenna, and G. Peyré. Iterative Bregman Projections for Regularized Transportation Problems. *SIAM Journal on Scientific Computing*, 37(2):A1111–A1138, 2015.
4. S. Borgwardt. Strongly Polynomial 2-Approximations for Discrete Wasserstein Barycenters. *eprint arXiv:1704.05491*, 2017.
5. S. Borgwardt and S. Patterson. Improved Linear Programs for Discrete Barycenters. *INFORMS Journal on Optimization*, forthcoming 2019.
6. G. Carlier, A. Oberman, and E. Oudet. Numerical methods for matching for teams and Wasserstein barycenters. *ESAIM: Mathematical Modeling and Numerical Analysis*, 49(6):1621–1642, 2015.
7. Michele Conforti, Gérard Cornuéjols, and Giacomo Zambelli. *Integer Programming*. Springer, 2014.
8. M. Cuturi. Sinkhorn Distances: Lightspeed Computation of Optimal Transportation Distances. *Advances in Neural Information Processing Systems*, (26):2292–2300, 2013.
9. M. Cuturi and A. Doucet. Fast Computation of Wasserstein Barycenters. In *Proceedings of the 31st International Conference on Machine Learning (ICML-14)*, pages 685–693. JMLR Workshop and Conference Proceedings, 2014.
10. George B. Dantzig and Philip Wolfe. Decomposition Principle for Linear Programs. *Operations Research*, 8(1):101–111, February 1960.
11. L. R. Ford and D. R. Fulkerson. Solving the Transportation Problem. *Management Science*, 3(1):24–32, 1956.
12. A. Kroshnin, D. Dvinskikh, P. Dvurechensky, A. Gasnikov, N. Tupitsa, and C. Uribe. On the Complexity of Approximating Wasserstein Barycenter. *eprint arXiv:1901.08686*, 2019.
13. J. Miller. *Transportation Networks and Matroids: Algorithms through Circuits and Polyhedrality*, 2016. Ph.D. thesis, University of California Davis.
14. Victor M. Panaretos and Yoav Zemel. Statistical Aspects of Wasserstein Distances. *Annual Review of Statistics and Its Application*, 6(1):405–431, 2019.
15. E. Tenetov, G. Wolansky, and R. Kimmel. Fast Entropic Regularized Optimal Transport Using Semidiscrete Cost Approximation. *SIAM Journal of Scientific Computing*, 40(5):3400–3422, 2018.

16. C. Villani. *Optimal transport: old and new*, volume 338. Springer, 2009.
17. L. Yang, J. Li, D. Sun, and K.-C. Toh. A Fast Globally Linearly Convergent Algorithm for the Computation of Wasserstein Barycenters. *eprint arXiv:1809.04249*, 2019.
18. J. Ye, P. Wu, J. Z. Wang, and J. Li. Fast Discrete Distribution Clustering Using Wasserstein Barycenter With Sparse Support. *IEEE Transactions on Signal Processing*, 65(9):2317–2332, 2017.
19. Yoav Zemel and Victor M. Panaretos. Fréchet means and Procrustes analysis in Wasserstein space. *Bernoulli*, 25(2):932–976, 2019.